
A fault slip model to study earthquakes due to pore pressure perturbations

A PREPRINT

Saumik Dana
University of Southern California
Los Angeles, CA 90007
sdana@usc.edu

Birendra Jha
University of Southern California
Los Angeles, CA 90007
bjha@usc.edu

April 14, 2021

ABSTRACT

The burgeoning need to sequester anthropogenic CO₂ for climate mitigation and the need for energy sustenance leading upto enhanced geothermal energy production has made it incredibly critical to study potential earthquakes due to fluid activity in the subsurface. These earthquakes result from reactivation of faults in the subsurface due to pore pressure perturbations. In this work, we provide a framework to model fault slip due to pore pressure change leading upto quantifying the earthquake magnitude.

1 Introduction

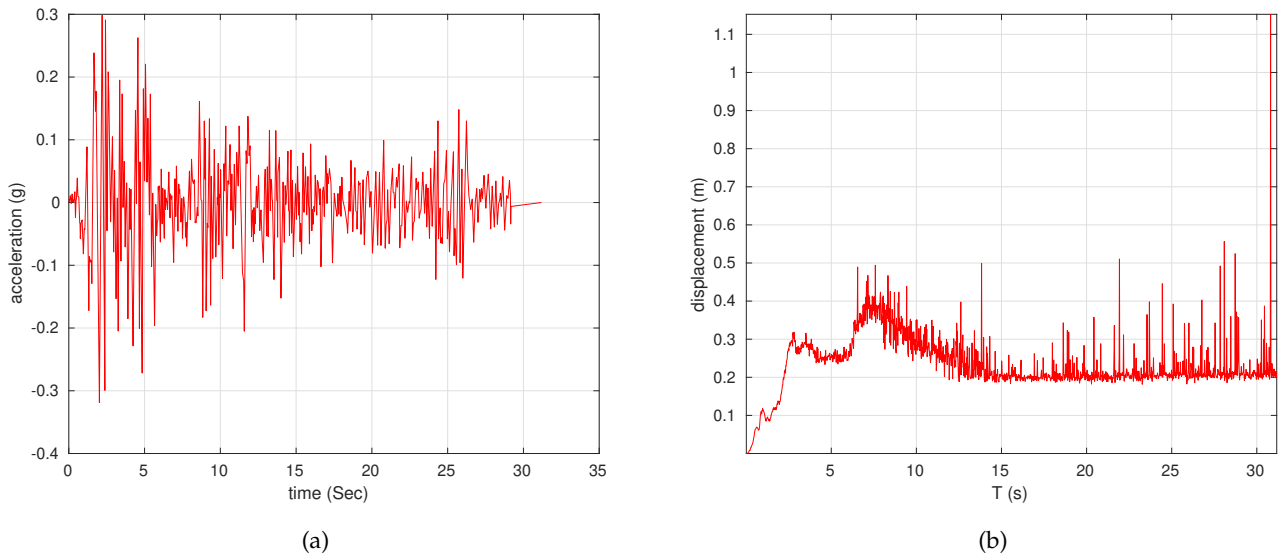


Figure 1: 1940 El Centro earthquake. (a) Accelerogram (measured as normalized to acceleration due to gravity $g = 9.8 \text{ m/s}^2$) and (b) Displacement Response Spectrum

Earthquakes occur as a result of global plate motion. Some plate boundaries glide past each other smoothly, while others are punctuated by catastrophic failures. Some earthquakes stop after only a few hundred metres while others continue rupturing for a thousand kilometres. The simplest model for earthquake initiation is to assume that when the stress accumulated in the plates exceeds some failure criterion on a fault plane, an earthquake happens [1]. Evaluating this criterion requires both a measure of the resolved stress on the fault plane and a quantifiable model for the failure threshold. The groundbreaking work of [2] started with the fact that any stress field can be completely described by its principal stresses, which are given by the eigenvectors of the stress tensor and are interpretable as the normal stresses in three orthogonal directions. He then proposed that: (1) the stress state could be resolved by assuming that one principal stress is vertical since the Earth's surface is a free surface and (2) faulting occurs when the resolved shear stress exceeds the internal friction on some plane in the medium. Internal friction is defined analogously with conventional sliding friction as a shear stress proportional to the normal stress on a plane. One complication to this simple picture was recognized early on. High fluid pressures can support part of the load across a fault and reduce the friction. The importance of the fluid effect on fault friction was first recognized by [3]. In the course of their work on oil exploration, they observed that pressures in pockets of fluids in the crust commonly exceeded hydrostatic pressure. They connected this observation with studies of faulting and proposed that the pore pressure at a depth can approach the normal stress on faults, resulting in low friction. Fig. 1 shows the seismograph recorded acceleration of the 1940 EL Centro earthquake that occurred in the Imperial Valley in southeastern Southern California near the USA-Mexico border. It was the first major earthquake to be recorded by a strong-motion seismograph located next to a fault rupture, and led to a total damage of \$6 million [4]. In section 2, we explain how the pore pressure enters into the computation of fault slip. In section 3, we explain the friction model and most popular empirical relations for quantifying earthquakes. Finally, in section 4, we provide conclusions and outlook for future work.

2 Fault slip model

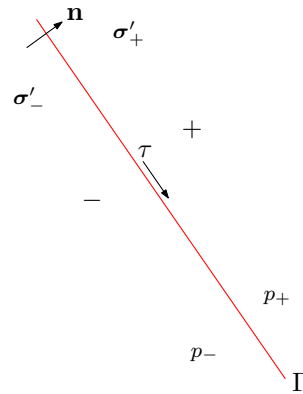


Figure 2: The two sides of the fault surface, which need not be planar, are designated as the '+' side and the '-' side

We treat faults as surfaces of discontinuity embedded in the continuum across which displacement is allowed to be discontinuous to recognize the possibility of fault slip [5, 6]. As shown in Fig. 2, the fault normal vector \mathbf{n} points from the negative side to the positive side of the fault. Slip on the fault is the displacement of the positive side relative to the negative side,

$$(\mathbf{u}_+ - \mathbf{u}_-) - \mathbf{d} = \mathbf{0} \text{ on } \Gamma, \quad (1)$$

where \mathbf{d} is the fault slip vector. We impose the effective traction on the fault by introducing a Lagrange multiplier, \mathbf{l} , which is a force per unit area required to satisfy Eq. (1). A positive value of $\mathbf{l} \cdot \mathbf{n}$ indicates that a tensile effective stress is transmitted across the fault surface. The Kuhn-Tucker conditions of contact mechanics are obeyed such that no penetration occurs and the effective normal traction stays compressive at the contact surface. The frictional stress τ_f on the fault as

$$\tau_f = \begin{cases} \tau_c - \mu \mathbf{l} \cdot \mathbf{n}, & \mathbf{l} \cdot \mathbf{n} < 0, \\ \tau_c, & \mathbf{l} \cdot \mathbf{n} \geq 0, \end{cases} \quad (2)$$

where τ_c is the cohesive strength of the fault and μ is the coefficient of friction. The shear traction on the fault is computed as

$$\tau = |\mathbf{l} - (\mathbf{l} \cdot \mathbf{n})\mathbf{n}|$$

We use the Mohr-Coulomb theory to define the stability criterion for the fault [7]. When the shear traction on the fault is below the friction stress, $\tau \leq \tau_f$, the fault does not slip. When the shear traction is larger than the friction stress, $\tau > \tau_f$, the contact problem is solved to determine the Lagrange multipliers and slip on the fault, such that the Lagrange multipliers are compatible with the frictional stress [5].

A difference in fluid pressure across the fault leads to a pressure jump $[[p]]_\Gamma = p_+ - p_-$, where p_+ and p_- are the equivalent multiphase pressures on the ‘positive’ and the ‘negative’ side of the fault. This pressure jump leads to a discontinuity in the effective stress across the fault, such that the total stress is continuous,

$$\boldsymbol{\sigma}'_- \cdot \mathbf{n} - b p_- \mathbf{n} = \boldsymbol{\sigma}'_+ \cdot \mathbf{n} - b p_+ \mathbf{n}, \quad (3)$$

where b is the Biot coefficient. Fault stability can be assessed by evaluating the stability criterion on both sides of the fault separately. The side of the fault where the criterion is met first determines the fault stability. Equivalently, this can be achieved by defining a *fault pressure* that is a function of the pressures on the two sides, p_+ and p_- . Introducing the fault pressure allows us to uniquely define the *effective* normal traction on the fault, σ'_n , and determine the fault friction τ_f (Eq. (2)). Since the stability criterion $\tau > \tau_f$ is first violated with the larger pressure, we define the fault pressure p as

$$p = \max(p_-, p_+). \quad (4)$$

3 Friction model and earthquake quantification

The rate- and state-dependent friction model [8, 9, 10, 11, 12] is

$$\begin{aligned} \mu &= \mu_0 + A \ln \left(\frac{V}{V_0} \right) + B \ln \left(\frac{V_0 \theta}{d_c} \right), \\ \frac{d\theta}{dt} &= 1 - \frac{\theta V}{d_c}, \end{aligned} \quad (5)$$

where $V = |d\mathbf{d}/dt|$ is the slip rate magnitude, μ_0 is the steady-state friction coefficient at the reference slip rate V_0 , A and B are empirical dimensionless constants, θ is the macroscopic variable characterizing state of the surface and d_c is a critical slip distance. Here, θ may be understood as the frictional contact time [8], or the average maturity of contact asperities between the sliding surfaces [13]. The evolution of θ is assumed to be independent of changes in the normal traction that can accompany the fault slip due to changes in fluid pressure. The model accounts for the decrease in friction (slip-weakening) as the slip increases, and the increase in friction (healing) as the time of contact or slip velocity increase. The two effects act together such that $A > B$ leads to strengthening of the fault, stable sliding and creeping motion, and $A < B$ leads to weakening of the fault, frictional instability, and accelerating slip. In this way, the

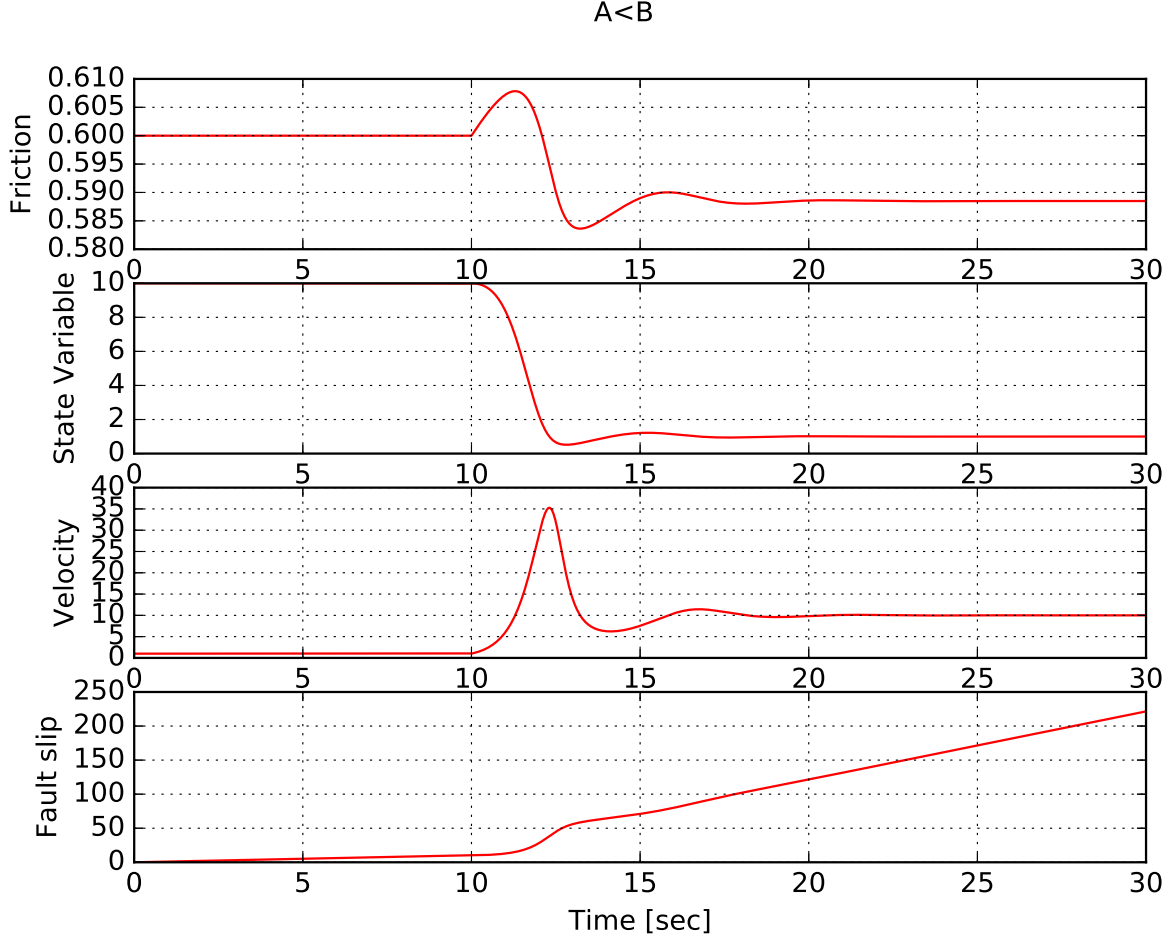


Figure 3: Slip weakening behavior with $A = 0.005$ and $B = 0.01$. Units of velocity and fault slip are $\mu m/s$ and μm respectively

model is capable of capturing repetitive stick-slip behavior of faults and the resulting seismic cycle [9, 11]. Eq. (5) can be written as

$$V = V_0 \exp \left(\frac{1}{A} \left(\mu - \mu_0 - B \ln \left(\frac{V_0 \theta}{d_c} \right) \right) \right), \quad (6)$$

$$\frac{d\theta}{dt} = 1 - \frac{\theta V}{d_c}$$

Following [14, 15, 16], we model a fault by a slider spring system. The slider represents either a fault or a part of the fault that is sliding. The stiffness k represents elastic interactions between the fault patch and the ductile deeper part of the fault, that is assumed to creep at a constant rate. This simple model assumes that slip, stress and friction law parameters are uniform on the fault patch. The friction coefficient of the block is given by

$$\mu = \frac{\tau}{\sigma} = \frac{\tau_l - k\delta}{\sigma} \quad (7)$$

where k is the spring stiffness, σ is the normal stress, τ the shear stress on the interface, τ_l is the remotely applied stress acting on the fault in the absence of slip, and $-k\delta$ is the decrease in stress due to fault slip.

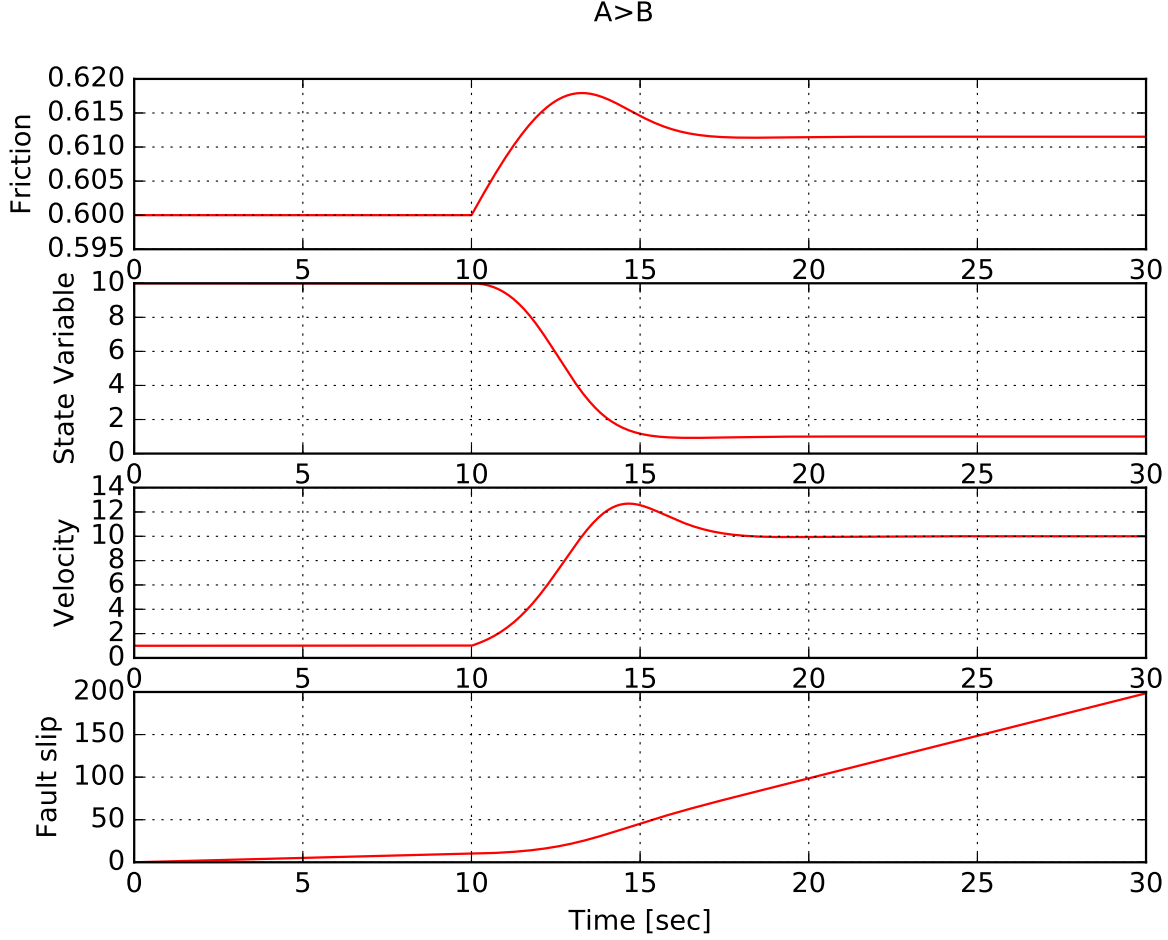


Figure 4: Slip strengthening behavior with $A = 0.01$ and $B = 0.005$. Units of velocity and fault slip are $\mu m/s$ and μm respectively

We consider the case of a constant stressing rate

$$\dot{\tau}_l = kV_l \quad (8)$$

where V_l is the load point velocity. The initial stress may be smaller or larger than steady state friction owing to coseismic slip on the fault patch or on adjacent parts of the fault. Expression (7) neglects inertia, and is thus only valid for low slip speed in the interseismic period. The stiffness is a function of the fault length l and shear modulus G [16]

$$k \approx \frac{G}{l} \quad (9)$$

In lieu of the above, we write

$$\begin{aligned} \frac{d\mu}{dt} &\approx \frac{G}{l\sigma}(V_l - V) \equiv k'(V_l - V), \\ \frac{dV}{dt} &= V \frac{d}{dt} \left(\frac{1}{A} \left(\mu - \mu_0 - B \ln \left(\frac{V_0 \theta}{d_c} \right) \right) \right) \equiv \frac{V}{A} \left(\frac{d\mu}{dt} - \frac{B}{\theta} \frac{d\theta}{dt} \right) \end{aligned} \quad (10)$$

As shown in Figs. 3 and 4, we plot the slip weakening and slip strengthening responses for $k' = 0.001[1/\mu m]$, $d_c = 10[\mu m]$, $\mu_0 = 0.6$, $V_0 = 1[\mu m/s]$ and the load point velocity taking a jump as follows

$$V_t = \begin{cases} 1[\mu m/s], & t < 10[s], \\ 10[\mu m/s], & t \geq 10[s] \end{cases} \quad (11)$$

3.1 Quantifying earthquake

The total amount of fault slip during the event is correlated to seismic magnitude. The seismic moment M_0 is a measure of the size and energy release of an earthquake [17]. M_0 is defined as the integral of fault slip over the fault area S times the shear modulus as

$$M_0 = G \int_{\Gamma} |\mathbf{d}| dS \approx G|\mathbf{d}|S \quad (12)$$

Although fault surface area can seldom be measured, several empirical relations make it possible to estimate it for faults for which the average slip is known. [18] successfully explained several empirically determined scaling laws of earthquakes using a model in which the surface area of slip is proportional to the square of average slip

$$S = \frac{\pi G^2}{4ec_2c_3} |\mathbf{d}| \quad (13)$$

where $c_2 \sim 2 \times 10^{-4} GPa^2 m^{-1}$ for faults with displacements ranging from 1 m to 10^5 m [19], $c_3 \sim 1/2$ and $e \sim 2$ [20]. From [21], the seismic moment magnitude M_w is defined as

$$M_w = \frac{\log_{10} M_0}{1.5} - 6.06 \quad (14)$$

where M_0 is defined in $N - m$.

4 Conclusions and outlook

We provided a framework in which the pore pressure changes are likely incorporated into the quantification of earthquakes triggered as a result of fluid injection and/or withdrawal in the subsurface. The rate and state model is the standard bearer for the friction evolution with fault slip. It is important to note that the slider spring model would be replaced by the output of the coupled flow and geomechanics simulator in our future works. The slider spring model, though, provides an excellent gauge for the potential earthquake response of the subsurface to stress perturbations. It is also important to note that the constant stress rate loading Eq. (8) is valid for low slip speeds in the interseismic period. It can be replaced by some other phenomenological models to study earthquake response for high slip speeds in the interseismic period. It is also important to note that the computation of fault shear stress can involve the use of a radiation term, especially in the context of enhanced geothermal energy production [22]. We shall study all these models as a part of future work.

References

- [1] Hiroo Kanamori and Emily E Brodsky. The physics of earthquakes. *Reports on Progress in Physics*, 67(8):1429, 2004.
- [2] Ernest Masson Anderson. The dynamics of faulting. *Transactions of the Edinburgh Geological Society*, 8(3):387–402, 1905.

- [3] M King Hubbert and William W Rubey. Role of fluid pressure in mechanics of overthrust faulting: I. mechanics of fluid-filled porous solids and its application to overthrust faulting. *Geological Society of America Bulletin*, 70(2):115–166, 1959.
- [4] Carl W Stover and Jerry L Coffman. *Seismicity of the United States, 1568-1989 (revised)*. US Government Printing Office, 1993.
- [5] Birendra Jha and Ruben Juanes. Coupled multiphase flow and poromechanics: A computational model of pore pressure effects on fault slip and earthquake triggering. *Water Resources Research*, 50(5):3776–3808, 2014.
- [6] Brad T Aagaard, Matthew G Knepley, and Charles A Williams. A domain decomposition approach to implementing fault slip in finite-element models of quasi-static and dynamic crustal deformation. *Journal of Geophysical Research: Solid Earth*, 118(6):3059–3079, 2013.
- [7] J. C. Jaeger and N. G. W. Cook. *Fundamentals of Rock Mechanics*. Chapman and Hall, London, 1979.
- [8] J. H. Dieterich. Modeling of rock friction, 1. Experimental results and constitutive equations. *J. Geophys. Res.*, 84:2161–2168, 1979.
- [9] J. H. Dieterich. Constitutive properties of faults with simulated gouge. *Mechanical Behaviour of Crustal Rocks: The Handin Volume, Geophys. Monogr. Ser.*, 24:108–120, 1981.
- [10] A. L. Ruina. Slip instability and state variable friction laws. *Geophys. Res. Lett.*, 88:359–370, 1983.
- [11] C. H. Scholz. Mechanics of faulting. *Ann. Rev. Earth Planet. Sci.*, 17:309–334, 1989.
- [12] C. Marone. Laboratory-derived friction laws and their application to seismic faulting. *Ann. Rev. Earth Planet. Sci.*, 26:643–696, 1998.
- [13] J. R. Rice. Spatio-temporal complexity of slip on a fault. *J. Geophys. Res.*, 98:9885–9907, 1993.
- [14] James R Rice and Ji-cheng Gu. Earthquake aftereffects and triggered seismic phenomena. *Pure and Applied Geophysics*, 121(2):187–219, 1983.
- [15] Ji-Cheng Gu, James R Rice, Andy L Ruina, and T Tse Simon. Slip motion and stability of a single degree of freedom elastic system with rate and state dependent friction. *Journal of the Mechanics and Physics of Solids*, 32(3):167–196, 1984.
- [16] James H Dieterich. Earthquake nucleation on faults with rate-and state-dependent strength. *Tectonophysics*, 211(1-4):115–134, 1992.
- [17] Seth Stein and Michael Wyssession. *An introduction to seismology, earthquakes, and earth structure*. John Wiley & Sons, 2009.
- [18] Hiroo Kanamori and Don L Anderson. Theoretical basis of some empirical relations in seismology. *Bulletin of the seismological society of America*, 65(5):1073–1095, 1975.
- [19] John J Walsh and Juan Watterson. Analysis of the relationship between displacements and dimensions of faults. *Journal of Structural geology*, 10(3):239–247, 1988.
- [20] JJ Walsh and J Watterson. Distributions of cumulative displacement and seismic slip on a single normal fault surface. *Journal of Structural Geology*, 9(8):1039–1046, 1987.
- [21] Thomas C Hanks and Hiroo Kanamori. A moment magnitude scale. *Journal of Geophysical Research: Solid Earth*, 84(B5):2348–2350, 1979.
- [22] Mark W McClure and Roland N Horne. Investigation of injection-induced seismicity using a coupled fluid flow and rate/state friction model. *Geophysics*, 76(6):WC181–WC198, 2011.